

Electron and Hole Transfer from Indium Phosphide Quantum Dots

J. L. Blackburn,* D. C. Selmarten, R. J. Ellingson, M. Jones, O. Micic, and A. J. Nozik

National Renewable Energy Laboratory, Golden, Colorado 80401

Received: July 20, 2004; In Final Form: November 24, 2004

Electron- and hole-transfer reactions are studied in colloidal InP quantum dots (QDs). Photoluminescence quenching and time-resolved transient absorption (TA) measurements are utilized to examine hole transfer from photoexcited InP QDs to the hole acceptor *N,N,N',N'*-tetramethyl-*p*-phenylenediamine (TMPD) and electron transfer to nanocrystalline titanium dioxide (TiO₂) films. Core-confined holes are effectively quenched by TMPD, resulting in a new ~4-ps component in the TA decay. It is found that electron transfer to TiO₂ is primarily mediated through surface-localized states on the InP QDs.

Introduction

Photosensitization of nanocrystalline titanium dioxide by semiconductor nanocrystals, or quantum dots (QDs), has received much attention.^{1–3} The energetic offset between the QD and TiO₂ conduction bands (CB) promotes charge separation, making such composites attractive for solar energy conversion and photocatalysis. The basic components of QD-sensitized TiO₂ solar cells are: (1) a high surface area nanoporous TiO₂ film on a conducting substrate, (2) a QD absorber layer adsorbed to the TiO₂ film by the appropriate technique, (3) a metallic counterelectrode, and (4) an appropriate hole conducting matrix to complete the circuit. Incident photons are absorbed by the QD layer, and the photoexcited electrons are transferred from the QD CB to the TiO₂ CB, where they diffuse through the TiO₂ network to the working electrode. The reducing species in the electrolyte solution neutralizes the oxidized QD, and itself is rereduced by electrons from the metallic counterelectrode.

The research on QD sensitization of high surface area TiO₂ electrodes builds on a wealth of research involving organic dyes as sensitizers. To date, the time scale of electron transfer, forward or reverse, from QDs into TiO₂, is poorly understood, though some reports are available.^{1,3,4} Transient absorption (TA) spectroscopy is a powerful tool capable of investigating ultrafast charge transfer across such interfaces, but very few TA studies of QD TiO₂ composites have been reported. Also important to understand is the hole transfer from photoexcited QD to an acceptor species. While solutions containing redox species such as the I⁻/I³⁻ couple have been used extensively for dye-sensitized titania solar cells, hole-conducting polymers are being examined as noncorrosive alternatives for this component.

In this paper, we examine electron and hole transfer from photoexcited InP QDs to titanium dioxide and to *N,N,N',N'*-tetramethyl-*p*-phenylenediamine (TMPD), respectively. We analyze these systems with photoluminescence (PL) spectroscopy and time-resolved TA spectroscopy in the visible and mid-infrared regions. Our results suggest that TMPD quenches the photogenerated hole in InP very effectively and introduce a rapid ~4-ps decay in the TA dynamics. PL results on InP–TiO₂ composites suggest that photogenerated electrons localized in InP surface states are efficiently injected into the conduction

band of TiO₂, while core-confined electrons are not injected efficiently. Dynamic TA results support the hypothesis that core-confined electrons are not injected into the TiO₂ conduction band.

Experimental Section

Indium phosphide QDs were synthesized by standard colloidal methods as previously reported.⁵ As-prepared QDs are capped with trioctylphosphine and trioctylphosphine oxide (TOP/TOPO); for hole-transfer studies, the TOP/TOPO capping groups were exchanged for TMPD.

Because the TOP/TOPO capping layer has been shown to inhibit charge transfer in QD/polymer conjugates⁶ and QD arrays,⁷ this capping layer was replaced with pyridine to make InP–TiO₂ composites. The pyridine-capped InP QDs were dissolved in toluene, because adsorption of the QDs to the TiO₂ surface was found to be slow and incomplete in pyridine, while adsorption in toluene was faster and more complete.²

TiO₂ and ZrO₂ nanocrystalline sol–gels were prepared by a method similar to that reported by Zaban and co-workers.⁸ For the TiO₂ colloids, 37 mL of titanium(IV) isopropoxide (Aldrich, 99.9%) in 10 mL of 2-propanol was slowly dripped over the course of 30 min into a stirred mixture of 80 mL of glacial acetic acid and 250 mL of deionized water at 0 °C. The resulting solution was heated to 80 °C for 8 h. It was then heated to 230 °C for 12 h in a titanium autoclave (Parr). Upon removal from the autoclave, the solution was sonicated for 5 min with a cell disrupter with an approximate power of 250 W to break up agglomerates. The solution was then concentrated to 150 g/L. Carbowax, at a ratio of 40 wt % (relative to TiO₂), was added to aliquots taken from this stock solution to produce a viscous sol–gel.

The ZrO₂ colloids were prepared in the same manner. The starting material was a 70 wt % solution of zirconium(IV) propoxide in 1-propanol (Aldrich). The autoclave temperature for the ZrO₂ colloids was 220 °C. In some ZrO₂ sol–gels, hydroxypropylcellulose was used as the polymer instead of Carbowax.

TiO₂ and ZrO₂ films were prepared by the following method. An area of the substrate is masked off with research-grade scotch tape. A small portion, typically less than 100 μL, of the sol–gel is pipetted onto the sapphire substrate between the two pieces of tape. A glass pipet is then used to drag the sol–gel across

* To whom correspondence may be addressed.

the substrate between the pieces of tape. The resulting film is allowed to dry in air and then placed in a furnace to heat at 450 °C for 1 h. This heating step removes the polymer from the film and sinters the colloids, producing a porous network of electrically contacted TiO₂ or ZrO₂ nanoparticles. Film thickness after sintering is typically 2–6 μm and may be increased by using multiple pieces of tape.

The QD–oxide electrodes were prepared by soaking the sintered TiO₂ or ZrO₂ films in the solution of pyridine-capped QDs in toluene. The soaking time to prepare optically dark electrodes varies from 24 h to one week, with higher QD concentration enabling shorter preparation times. In ref 2, thiolactic acid was found to enhance adsorption. We have found no appreciable difference of adsorption kinetics or electron-transfer behavior for bare TiO₂ films and TiO₂ films treated with thiolactic acid. All electrodes discussed in this report were prepared without the use of thiolactic acid as a linker molecule. We also stress here that, for purposes of comparison, InP–TiO₂ electrodes and InP–ZrO₂ electrodes were made from two aliquots of the same sample. Thus, no differences in processing exist for QDs adsorbed to TiO₂ or ZrO₂. This allows us to attribute differences in luminescence or TA dynamics to interactions with the substrate (e.g., charge transfer) and rules out that these effects may be attributed to differences in processing.

Steady-state absorption measurements were made using a Cary 500 double-beam spectrometer at a spectral resolution of 1 nm.

PL spectra were recorded using a Fluorolog-3 (JYHoriba) spectrometer that utilizes a charge-coupled device (CCD) detection system. Monochromatic excitation light was generated by a Xe arc lamp with a double monochromator. Fluorescence light was collected in right-angle mode for solutions and front-face mode for films. Fluorescence is passed through a single monochromator containing a 150 line/mm grating and imaged on the liquid nitrogen cooled CCD array. All PL spectra were corrected for the spectral output of the excitation source and for the spectral response of the detection optics.

The TA setup is based on a Clark-MXR CPA-2001 regeneratively amplified Ti:sapphire laser, operating at 989 Hz and 775 nm. The ~125-fs duration, 775-nm pulses from the CPA-2001 were used to pump visible and infrared optical parametric amplifiers (OPAs). The visible OPA is a TOPAS from Quatronix, capable of output in the range of 290 nm to 2.4 μm. The IR OPA (Clark-MXR) provides tunable near-IR pulses from 1.1 to 2.5 μm; the signal and idler pulses from the IR OPA were combined in a AgGaS₂ crystal to generate mid-IR probe pulses tunable from 3 to 6 μm by difference frequency generation. Spatially filtering the visible pump beam was used to improve the transverse mode quality.

For dynamic measurements, the wavelength of interest was set by the monochromator and the pump–probe delay was varied. Spectral data were obtained by maintaining a fixed pump–probe delay while spectrally dispersing the probe beam; all spectral data were corrected for the chirp of the probe.

Results and Discussion

Hole Quenching in InP Quantum Dots.

The TOP/TOPO capping groups of as-prepared InP QDs may be exchanged for other capping groups to modify the electronic properties of the QDs. For example, when the capping group is changed from TOP/TOPO to *N,N,N',N'*-tetramethyl-*p*-phenylenediamine (TMPD), the QD luminescence is completely quenched. Figure 1 compares the PL spectra of TOPO-capped

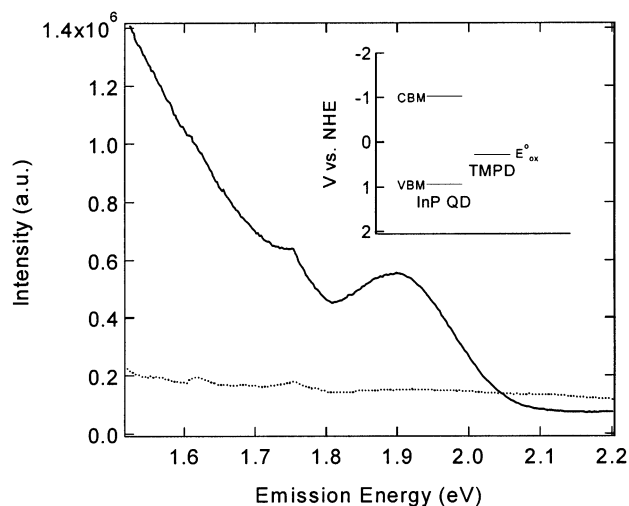


Figure 1. PL spectra of TOP/TOPO (solid line) and TMPD (dotted line) capped InP QDs. Inset shows approximate energy levels of QDs and TMPD.

and TMPD-capped 36-Å InP QDs. It is clearly seen that the TMPD cap completely quenches the QD PL. This is due to the relative energetics of the QD valence band and the oxidation potential (E_{ox}^o) of the TMPD molecule,⁹ which make TMPD a good hole scavenger for the photoexcited InP QDs.

The conduction and valence band positions of the InP QDs are estimated using a simple effective mass calculation which weights the amount of the confinement energy given to the conduction and valence bands according to the electron and hole effective masses¹⁰

$$\Delta E_{CB} = \Delta E_{con} \left(\frac{m_h^*}{m_h^* + m_e^*} \right) \quad (1)$$

In eq 1, ΔE_{CB} is the energy change of the conduction band, ΔE_{con} is the total confinement energy calculated as ($E_{1S} - E_g$) where E_{1S} is the lowest energy excitonic transition of the QD and E_g is the bulk band gap of InP (1.35 eV), and m_h^* and m_e^* are the hole and electron effective masses, respectively. According to eq 1, for the 36-Å InP QD shown in Figure 1, the conduction band shift for the InP QD is ~540 meV, meaning the valence band shifts ~94 meV. By use of the value of -0.5 V vs the normal hydrogen electrode (NHE) for the conduction band redox potential for bulk InP and +0.85 V vs NHE for the bulk valence potential,¹¹ the QD redox potentials are -1.04 V (CB) and +0.944 V (VB) vs NHE. The one-electron oxidation potential of the TMPD has been measured by cyclic voltammetry (CV) and found to be ~-0.28 V vs ferrocene (~+0.27 V vs NHE).^{9,12} A schematic showing the energetics of the TMPD–InP system is shown in the inset of Figure 1. Quenching of the QD PL is achieved following photoexcitation when an electron from the TMPD HOMO is injected into the valence band of the InP QD.

TA measurements were performed on the TOP/TOPO- and TMPD-capped samples shown in Figure 1 to examine the effect of hole trapping on the dynamics. Part a of Figure 2 compares the 1S visible bleaching and mid-IR dynamics for the 36-Å InP QDs pumped at 600 nm. The bleach is measured at 625 nm, the position of the lowest (1S) excited state (Figure 2b). The mid-IR wavelength is chosen to correlate with the energy spacing between the 1S and 1P excitonic states, ~330 meV. The main effect of changing the capping group from TOP/TOPO to TMPD is the introduction of a ~4-ps relaxation component

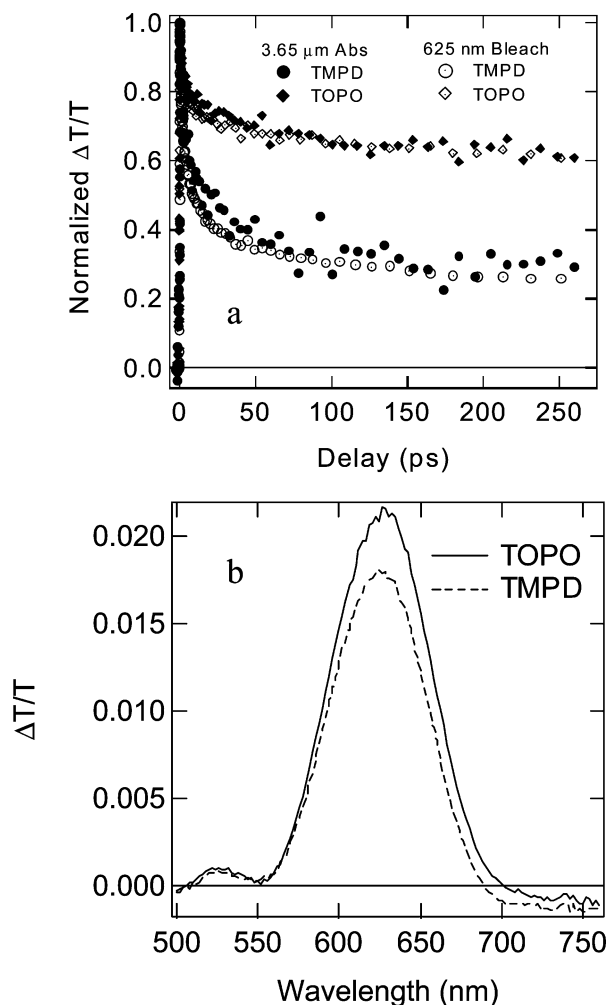


Figure 2. (a) Comparison of visible bleach and mid-IR absorbance dynamics for ~ 36 -Å InP QDs dispersed in hexane and pumped at 600 nm. (b) TA spectra for the same sample, taken at 10 ps, excited at 460 nm. For both experiments, the average number of excitons excited per QD, $\langle N_0 \rangle = 0.25$ – 0.30 .

in the TMPD-capped sample, indicating a much faster depopulation of the lowest excited state.

To analyze the meaning of this fast decay for the TMPD-capped QDs, we must consider the origin of the TA bleach. Following photoexcitation, occupation of discrete excited states, or state filling, leads to absorption bleaches at the positions of these excited states in the TA spectrum. The bleach from state filling results from a decrease in oscillator strength for the occupied excited states. We must also consider the contribution of Coulomb interactions to the TA signals. Photoexcitation of carriers in semiconductor QDs generates local electric fields, which modulate the optical absorption spectrum by the Stark effect.^{13–16} For charge-transfer systems, we must also consider fields created as a result of charge separation. The Stark effect is well characterized and is distinguished by a TA bleach spectrum with maxima and minima correlated to the derivative of the linear absorption spectrum.¹³ From Figure 2b, it is evident that the spectrum for the TMPD-capped QDs lacks the characteristic derivative-like features that would indicate the influence of field effects. This suggests that any bleach contribution of a charge-transfer-induced Stark effect is minor compared to the bleaching arising from state filling. Thus, we conclude that state filling dominates the TA signals that we measure, and therefore the rapid 4-ps decay induced by TMPD will be analyzed in accordance with state filling.

We now must analyze the contribution of both the electron and hole to the TA signals. In most reports, the electron is considered to be the dominant species measured by the visible bleach due to the spread of the hole occupation numbers over several valence levels within kT of each other.¹⁴ Also, the mid-IR absorbance is typically attributed to the transition of the photoexcited electron from the lowest conduction level ($1S_c$) to the second conduction level ($1P_c$).¹⁷ These assignments suggest that the dynamics of the visible bleach measure the same species as the dynamics of the mid-IR absorbance. In ref 18, the effects of electron and hole scavengers on the TA dynamics for CdSe QDs were examined. The first finding of this report was that the dynamics of the visible bleach are indeed closely correlated to the dynamics of absorbance in the mid-IR, suggesting they do measure the same species. Clearly, the visible and mid-IR dynamics for the TOP/TOPO and TMPD-capped dots match very well, showing that this correlation also holds for InP QDs. This correlation also shows that QD charge-transfer reactions may be monitored in both spectral regions.

The next finding of the report by the El-Sayed group¹⁸ relates to the contribution of both carriers to the visible bleach and mid-IR absorbance. By assumption of a complete removal of conduction band electrons in CdSe QDs by the electron scavenger benzoquinone, the measurements showed that while the majority of the signal in the visible and mid-IR could be attributed to the electron, the contribution of the hole to both signals is also significant. Bleach dynamics were also used to successfully follow hole relaxation in $\text{Cu}_{1.8}\text{S}$ QDs treated with benzoquinone.¹⁹ However, it must be noted that, in a separate report, the same group analyzed the effect of a hole-scavenging molecule on the visible bleach dynamics for CdSe QDs and quantum rods (QRs) based entirely on electrons.²⁰ In this report, the large effect that the adsorbed hole scavenger had on the visible bleaching dynamics was attributed to a modified coupling of the electronic excitation to vibrations of the capping molecule. It is emphasized that the effect of TMPD on our InP TA dynamics agrees with the results of ref 20, which shows that the 1S bleach decay is dramatically faster when the hole acceptor *n*-butylamine is adsorbed to the CdSe QD. To the contrary, in ref 18, the thiophenol hole-scavenging molecule dramatically *lengthens* the 1S bleach decay. In light of these contradictory results, determining the relative contributions of electrons and holes to the visible bleach and mid-IR absorbance remains a challenge.

If we assume that the visible bleach and mid-IR absorbance are only due to state filling of *electron* levels, we may come to two conclusions. One is the possibility of TMPD acting as an electron scavenger. If this were the case, the ~ 4 -ps decay could be directly attributed to electron removal from the conduction band of the InP QDs. In this scenario, we would expect the TMPD reduction potential to fall between the QD CB and VB. However, TMPD is one of the most well characterized electron *donors*, and we have found no reports in which TMPD acts as an electron *acceptor*. Likewise, the oxidation potential of TMPD makes it an ideal electron donor for InP QDs, as shown in Figure 1. We therefore find little support for the idea that the observed change in dynamics is due to the TMPD capping molecules acting as electron scavengers.

The other conclusion based on the sole contribution of electrons is that the vibrational characteristics of the adsorbed TMPD molecules greatly increase the rate of recombination in the InP QD. This has been suggested for the hole scavenger *n*-butylamine (*n*-BA) on CdSe QDs.²⁰ In that case, it was suggested that the rapid 1S bleach decay for *n*-BA capped QDs

resulted from the efficient coupling of the remaining CB electron to vibrations of the capping molecule. In this scenario, the excited electron may couple to the large number of vibrational modes of the capping molecules, opening up an efficient nonradiative pathway for relaxation and recombination of the conduction band electron. In our case, because the early time 1S dynamics are fit by ~ 100 ps for the TOPO-capped QDs and ~ 4 ps for the TMPD-capped QDs, this would suggest a dramatic difference in electronic coupling to the two different caps. While recent evidence has suggested that electronic coupling to the capping molecules may be significant,²¹ the extent to which this coupling should differ among different capping molecules is unclear. Important factors should be the specific vibrational structure of the ligands as well as the rotational degrees of freedom, which will determine how efficiently the ligands may reorient in response to the charge redistribution. The measurement of this coupling strength has been performed by three-pulse echo peak shift spectroscopy,²¹ which is outside the scope of our current experimental capabilities. Thus, although we do not feel that we have enough evidence to claim that coupling of the electron to the ligands is responsible for the rapid 1S bleach decay for our TMPD-capped InP QDs, we cannot rule this possibility out. The coupling of the electron to vibrations of the surrounding media (solvent, cap) is a concept that is beginning to receive much-needed attention.

If we consider the hole dynamics to be directly observable in the TA dynamics, then the faster 1S bleach decay for the TMPD-capped QDs could represent the removal of the hole from the valence band by TMPD. This would indicate a ~ 4 -ps hole transfer from the InP QD to TMPD. For this scenario, the hole must contribute to both the visible bleach and mid-IR absorbance, such that its removal from the valence band would result in a decrease in the magnitude for both signals. As mentioned above, evidence for hole contribution to both signals has been seen for CdSe and $\text{Cu}_{1.8}\text{S}$ QDs.^{18,19} In both of these experiments, incomplete decay of the bleach in the presence of the benzoquinone electron quencher suggests that the remaining hole does indeed contribute to the bleach signal. On the basis of this evidence, it is quite reasonable to conclude that the hole population in our InP QDs may be followed by the TA bleach and the matching mid-IR absorbance dynamics. We may also approach this problem from the other way around, using *our* results on InP QDs to suggest that, while the electron should dominate both signals, they may also have some contribution from the hole. The complete quenching of the PL indicates a complete removal of one charge carrier species, and as discussed above, it is highly improbable that TMPD could act as anything but a hole scavenger for InP QDs. Concomitant with the quenching of the PL, due to extraction of the hole, is a rapid ~ 4 -ps decay in the TA dynamics. One feasible conclusion from these data is that the hole contributes to the TA bleach and IR absorbance signals for photoexcited InP QDs, and the hole transfer event is directly observable from the TA dynamics.

Results such as the ones described above for TMPD hole quenching defy an easy or unambiguous treatment in the context of the prevailing theories for the TA bleach signal. Thus, more rigorous theoretical calculations and experimental measurements of electronic coupling to the media surrounding the QDs, as well as more selective carrier quenching experiments, could provide valuable insight. However, one important implication of these results is that charge-transfer reactions may be monitored in both the visible and mid-IR regions of the spectrum. Because the oxidized form of TMPD does not absorb in the mid-IR, the mid-IR and visible dynamics are closely

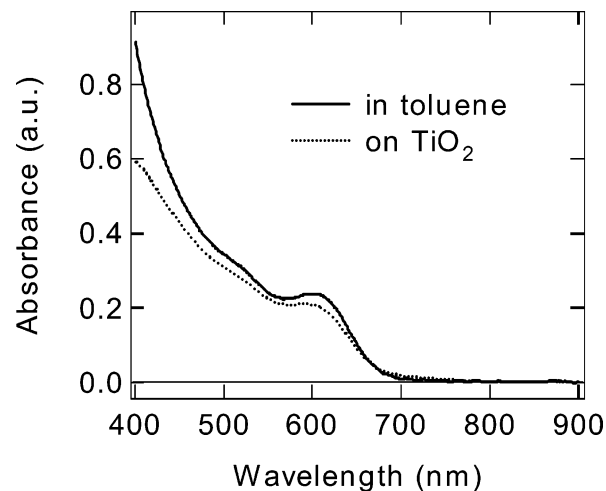


Figure 3. Absorbance spectra of 34-Å pyridine-capped InP QDs dispersed in toluene and adsorbed to TiO_2 film.

correlated for TOPO and TMPD-capped InP QDs. This is a very important consideration when attempting to measure charge-transfer reactions in which both the donor and acceptor species absorb in the mid-IR. For example, this comparison was recently utilized by our group to observe the rise time of the injected electron in CdS-sensitized TiO_2 composites.¹

Electron Transfer in InP– TiO_2 Composites.

We now focus on electron transfer from InP QDs adsorbed to high surface area titanium dioxide films. Soaking a sintered TiO_2 film in a concentrated solution of InP QDs produces a dark but optically transparent film. The absorption spectra of 34-Å pyridine-capped InP QDs in toluene and adsorbed to TiO_2 are shown in Figure 3. The fact that we observe the preservation of the excitonic structure emphasizes the well-defined nature of the QDs studied in these experiments. Also informative is the lack of a red-shift or spectral broadening of the 1S absorption peak, which indicates the absence of QD–QD coupling observed in close-packed QD arrays.⁷ This effect could be important if several monolayers of QDs adsorbed to the film. This also suggests a weak coupling between the QD excited states and TiO_2 acceptor states. The sharp features in the absorption spectrum become less pronounced if the sample is exposed to air due to the formation of an oxide layer on the surface of the QDs.²² We note, however, that exposure of the InP– TiO_2 composite to air is important for film stability under illumination, suggesting that oxidation of the InP surface protects the QDs from photocorrosion.

Parts a and b of Figure 4 show static PL spectra for ~ 40 -Å InP QDs coupled to nanocrystalline TiO_2 and ZrO_2 , respectively. Because of nonequivalent collection efficiencies, Figure 4 is only useful in comparing the shape of the PL spectrum, which should yield information on the spectral regions where quenching occurs. This experiment does not give information on PL quantum yields, either absolute or relative.

When the QDs are coupled to ZrO_2 , electron transfer is thermodynamically unfavorable, and hence, the PL spectrum should maintain the same shape that it has when the dots are dispersed in solution (inset). This is indeed the case, indicating that ZrO_2 is a good control substrate. Band gap PL can be seen in the region of 1.83 eV as a Gaussian peak with width (~ 200 meV) determined by the size distribution within the QD sample. This intrinsic QD luminescence arises from electrons that have thermalized to the CB edge recombining with thermalized holes in the VB.

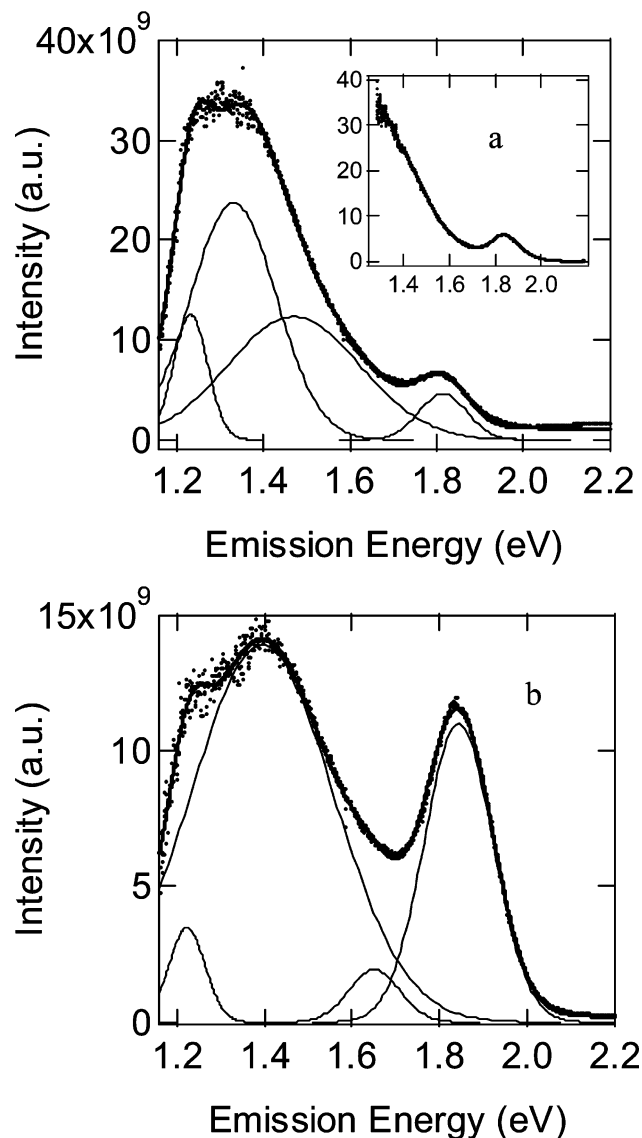


Figure 4. Multiple Gaussian fitting of PL spectra for (a) InP–ZrO₂ (mainframe) and (b) InP–TiO₂. Inset of (a) shows PL spectra of same InP QDs dispersed in toluene. Excitation is at 500 nm. Points show experimental data, thin solid lines show individual Gaussian components, and the dark solid line shows fit obtained by summing the individual components.

At lower energies, several different recombination pathways involving trap states exist: (1) recombination of a CB electron with a trapped hole; (2) recombination of a trapped electron with a VB hole; (3) recombination of a trapped electron with a trapped hole. We refer to this region as trap-state PL. Superimposed on the low-energy side of the band gap PL and steadily rising into the infrared is the broad spectrum representative of trap-state PL. The spectral broadness in this region arises from the variety of different recombination mechanisms that give rise to the PL, as well as the energetic dispersion of trap states within the QD sample. This broad trap-state emission peaks around 1.3 eV.

The CB offset in InP–TiO₂ composites is such that electron transfer from photoexcited InP QDs to the TiO₂ films is thermodynamically favorable. Luminescence from the InP–TiO₂ composite shows a much different spectral shape than the InP–ZrO₂ composite. Whereas the shape of the band gap PL is identical to that of the dots on ZrO₂, the trap-state PL has been dramatically quenched. Thus, an interaction of the QDs with the TiO₂ nanocrystals has quenched the trap-state emission of

the QDs. A mechanism that is consistent with this observation is that, in some photoexcited QDs, electrons become trapped in surface states and are transferred to the TiO₂ conduction band, making them unavailable to contribute to the trap-state PL. The lack of significant band gap PL quenching implies that a low percentage of core-confined electrons are transferred to TiO₂. Compare this figure, for example, to Figure 1, in which TMPD completely quenches the band-gap PL by removal of the core-confined hole. Thus, we expect the TA dynamics for the 1S transition to be little affected by the presence of the TiO₂ acceptor.

To make the case that electron transfer quenches the trap-state PL, we must rule out the scenario that the titanium dioxide nanoparticles efficiently passivate the surface of the InP QDs. In this scenario, the titanium dioxide nanoparticles would bind strongly to a large portion of the QD surface, tying up surface-dangling bonds. This passivation would enhance band gap emission and quench the deep trap emission, similar to what is seen when InP QDs are etched in a dilute solution of HF.²³ Also, media changes have been shown to enhance CdS QD emission in CdS/TiO₂ aqueous suspensions.²⁴ We dismiss this possibility, however, based on the static environment of our TiO₂ films as well as the average pore size in the film. In the above-mentioned experiments based on colloidal suspensions, dynamic rearrangement of the solute, solvent, and surfactant molecules can occur to give efficient surface passivation of the QDs. In a film, however, this type of rearrangement is not possible, and surface passivation by the TiO₂ nanoparticles should be strictly determined by the geometry of the sintered TiO₂ film. The average TiO₂ particle diameter used in these studies is ~25 nm. It has been shown for sintered TiO₂ films that the most probable pore size is ca. 30–40% larger than the average particle size and that ~80% of the pores are larger than the average particle size.²⁵ We therefore expect that the majority of the pore diameters in the films discussed here range from 25 to 35 nm. This, in turn, implies that, when an InP QD ($d = 3\text{--}4$ nm) intercalates into a pore in the film, it will most likely be in contact with only one or two TiO₂ particles. This is a much different physical environment than which would be required for an efficient surface passivation by the TiO₂ particles, namely, that of a large surface area of contact around the entire surface of the InP QD. We, therefore, dismiss the surface passivation scenario, and continue to discuss the results based on QD to TiO₂ electron transfer.

While the trap-state PL is dramatically quenched, some nonzero signal still remains. This is likely a result of two factors. One is a nonunity efficiency for electron injection from the electron trap states. Another factor is that one of the major pathways producing this trap-state emission should still prevail for QDs in which the electron remains in the QD CB. If it is inferred from the lack of significant band gap PL quenching that few CB electrons are transferred to TiO₂, then a CB electron recombining with a trapped hole is still a valid recombination pathway that will contribute to the trap-state PL. As it is very difficult to estimate the relative magnitude of the trap-state PL arising from QDs undergoing this recombination pathway, it remains a challenge to calculate an accurate charge-transfer efficiency.

However, an estimate is attempted by deconvoluting the area under the PL curves for the InP–ZrO₂ and InP–TiO₂ traces. This deconvolution is shown in Figure 4. The trap-state PL is most effectively fit by a sum of three Gaussians, and the band gap PL is fit by a single Gaussian with width of ~20 meV. The area under the PL curve in each region is proportional to

the number of QDs emitting in that region. However, non-equivalent collection efficiencies for the InP–TiO₂ and InP–ZrO₂ films prohibit us from directly comparing the two PL spectra. We therefore need some form of normalization, which we take as the band gap PL peak. A simple estimate of the quenching of the trap-state PL may be made by comparing the ratio of the total area for the band gap PL to the trap-state PL ($A_{\text{Eg}}/A_{\text{tr}}$) for both cases. For the InP–ZrO₂ sample, this value is 0.059 ± 0.009 , and for the InP–TiO₂ sample, this is 0.386 ± 0.034 . These values were calculated by fitting 13 spectra, exciting from 400 to 520 nm for both the InP–TiO₂ and InP–ZrO₂ sample, and averaging. If we assume no quenching or enhancement of the band gap PL, then the approximate quenching of the trap-state PL by TiO₂ is $1 - (0.059/0.386)$, or 0.85 ($\sim 85\% \pm 4\%$). TA results, discussed shortly, support the assumption of insignificant quenching of the band gap PL. Because the area under the PL curve in each region is proportional to the number of QDs emitting in that region, this calculation suggests that $\sim 85\%$ of the QDs that would normally emit via recombination of trapped carriers have instead transferred their electrons to TiO₂ and do not contribute to the emission spectrum. This estimate implies that the efficiency of charge transfer is rather high when the electron becomes localized at the surface of the QD.

A variety of different sizes of InP QDs have been examined to determine if the size-dependent energetics of the QD conduction band and/or trap-state energies will have an effect on the QD–TiO₂ interaction. The effect of adsorption to TiO₂ is the same in all cases: the trap-state PL is quenched while the band gap PL is unaffected. This suggests that electron injection from the QD surface states is the dominant mechanism for charge transfer in the entire size range studied, 26–50 Å.

To determine if the core-confined electrons are indeed little affected by TiO₂, we performed time-resolved TA measurements on the InP–TiO₂ composites. The first TA experiment consisted of a visible pump pulse (500 nm) followed by a white light probe pulse set to be resonant with the lowest excited state (1S) of the InP QD. For the ~ 36 -Å QDs studied here, the 1S peak occurs at ~ 620 nm. Since electron transfer to TiO₂ represents a new pathway for electrons to depopulate the 1S_e level, probing at the energy of the 1S transition should be able to monitor this process if it occurs.

The results of the pump–probe experiment are shown in part a of Figure 5. The completely uncoupled dots are represented by the toluene sample. Here, the dots are simply dispersed in toluene and have no other species with which to interact. The 1S bleach decays with time constants of 50 and 650 ps. When the QDs are coupled to TiO₂, the possibility for electron transfer now exists. It can be seen in Figure 5a that, when the QDs are coupled to TiO₂, the dynamics are largely unchanged. The faster time constant is slightly reduced to 28 ps, but the longer component is unaffected.

To determine whether the reduction of the fast time constant is due to the electron transfer between the QD and the TiO₂, we compare this result to the dynamics of the same dots coupled to ZrO₂. It is immediately apparent that the bleach dynamics are very similar on TiO₂ and ZrO₂, and indeed the kinetic fit yields time constants of 26 and 710 ps. Because the fast component is the same on both TiO₂ and ZrO₂ substrates (26 and 28 ps), this component cannot be attributed to an electron transfer event, and is likely a result of the different dielectric environment the QDs experience in the oxide films versus being solvated in toluene. Because the TA dynamics are largely unaffected by adsorption to TiO₂, these data suggest that

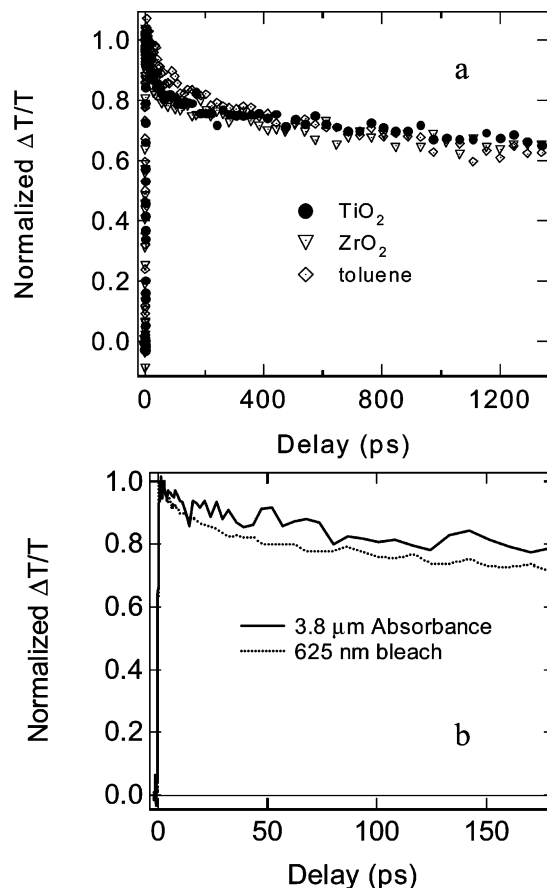


Figure 5. (a) Pump–probe TA experiment on ~ 36 -Å InP QDs in toluene, on TiO₂ film, and on ZrO₂ film. Samples are pumped at 500 nm and probed at the peak of the 1S bleach (620 nm). Biexponential fits to each decay give: toluene (50 ps, 650 ps); TiO₂ (28 ps, 600 ps); ZrO₂ (26 ps, 710 ps). (b) Comparison of mid-IR and visible bleach dynamics for the same InP–TiO₂ sample following excitation at 500 nm.

electrons are not transferred from the core 1S_e level of the QDs, consistent with the PL results discussed earlier.

To further analyze the electron transfer between the InP QDs and TiO₂, TA experiments were performed in the mid-IR range. In semiconductors, free carriers show pronounced absorption in the IR region, characterized generally by a monotonically rising response that may be approximated by λ^p , where p ranges from ~ 1.5 to 3.5 and λ is the photon wavelength.²⁶ While free electrons in the conduction band of TiO₂ should adhere to this model, the mid-IR signal in the InP QD is due to the strong intraband 1S–1P transition.²⁷

We have shown previously that a comparison of the visible bleaching and mid-IR dynamics is useful for extracting information about electron transfer from QDs to TiO₂. As discussed in ref 1, the bleach in the visible range should be sensitive only to the presence of the exciton in the lowest excited state of the InP QD. As shown in Figure 2, in the absence of an acceptor species whose reduced or oxidized form absorbs in the mid-IR, the visible bleach and mid-IR dynamics should match. However, when the InP QDs are coupled to TiO₂, a mid-IR absorbance signal will be measured from photoexcited excitons in the InP QDs and electrons injected into the TiO₂ conduction band. Thus, for InP–TiO₂, the signal measured in the mid-IR will be comprised of the decay of the InP exciton and a rise time associated with electron arrival in the TiO₂. Thus, a comparison of the visible bleach to the mid-IR absorbance may yield information on the InP–TiO₂ charge-transfer event.

We measured the visible bleaching dynamics and mid-IR absorbance dynamics for 36-Å InP QDs on TiO₂. The results of this comparison are shown in Figure 5b. While the bleach dynamics and mid-IR dynamics appear similar, a small but reproducible positive offset is seen for the IR dynamics. As discussed above, this offset is due to the electrons injected into the TiO₂ conduction band, which absorb at 3.8 μm. Because of the noise in the data, and since the offset is rather small, it is difficult to extract a time constant for electron transfer from these data.

The above PL and TA results may be rationalized by considering the thermodynamics of the InP–TiO₂ electron transfer. Temperature-dependent PL measurements indicate that while the trapping process for electrons in InP QDs is only mildly activated (100–200 J/mol), the barrier to detrapping is quite large, and greater than kT at room temperature (~5.4 kJ/mol for a 43-Å QD).²⁸ This large barrier to detrapping implies that, if electrons are trapped in surface states, they are more likely to recombine directly (radiative or nonradiative) than they are to thermally repopulate the conduction band. In the case where the surface-trapped electron “sees” an electron acceptor such as TiO₂, the electron-transfer reaction will proceed based on the relative kinetics of the radiative decay, nonradiative decay, and electron injection processes. This consideration explains why the electron-transfer event is observable in the PL measurements, but not in the TA measurements. If a thermal equilibrium existed between the 1S_e electron level and the surface electron trap states, electron transfer from the trap states would affect the observed lifetime of the 1S_e level and could be measured in the TA dynamics.

We also consider the barrier to electron injection from surface states and core-confined electron levels. Here, we turn to experiments on charge transport in close-packed CdSe QD arrays.²⁹ In these experiments, charge transfer occurs via field-assisted quantum mechanical tunneling between the isoenergetic single particle levels of individual CdSe QDs. It was found that the applied bias caused the QD deep trap PL to quench long before significant quenching of the band gap PL. This result was consistent with the theoretical calculation of the energy cost for charge separation, which showed that the energy cost for separating a surface-localized e⁻/h⁺ pair is approximately three times less than the energy cost for separating a core-confined e⁻/h⁺ pair. These findings are consistent with the findings of our group for photoexcited InP QDs, which show significant quenching of trap-state PL by the TiO₂ acceptor and insignificant quenching of the band gap PL.

Summary

We have examined electron and hole transfer from colloidal InP QDs with photoluminescence and transient absorption spectroscopy. We find that TMPD effectively scavenges the photogenerated hole in InP, quenching the QD luminescence. This hole-transfer event introduces a rapid ~4-ps component to the TA dynamics, which is observed in the dynamics of both the visible bleach and mid-IR absorbance. Electron transfer from

InP QDs to TiO₂ occurs primarily from trap states on the surface of the QDs. No evidence is found for electron injection from core-confined levels of the QDs. These results should be useful for further studies on QD-sensitized titanium dioxide composites and QD charge-transfer studies in general.

Acknowledgment. All authors wish to thank the U.S. Department of Energy, Office of Basic Energy Sciences, Division of Chemical Sciences, Geosciences, and Biosciences for financial support. Don Selmarten was supported by the Xcel Energy Renewable Development Fund.

References and Notes

- (1) Blackburn, J. L.; Selmarten, D. C.; Nozik, A. J. *J. Phys. Chem. B* **2003**, *107*, 14154.
- (2) Zaban, A.; Micic, O. I.; Gregg, B. A.; Nozik, A. J. *Langmuir* **1998**, *14*, 3153.
- (3) Plass, R.; Pelet, S.; Krueger, J.; Gratzel, M.; Bach, U. *J. Phys. Chem. B* **2002**, *106*, 7578.
- (4) Gopidas, K. R.; Bohorquez, M.; Kamat, P. V. *J. Phys. Chem.* **1990**, *94*, 6435.
- (5) Micic, O. I.; Cheong, H. M.; Fu, H.; Zunger, A.; Sprague, J. R.; Mascarenhas, A.; Nozik, A. J. *J. Phys. Chem. B* **1997**, *101*, 4904.
- (6) Greenham, N. C.; Poeng, X.; Alivisatos, A. P. *Phys. Rev. B* **1996**, *54*, 17628.
- (7) Micic, O. I.; Ahrenkiel, S. P.; Nozik, A. J. *Appl. Phys. Lett.* **2001**, *78*, 4022.
- (8) Zaban, A.; Ferrere, S.; Sprague, J.; Gregg, B. A. *J. Phys. Chem.* **1997**, *101*, 55.
- (9) Rawashdeh, A. M. M.; Sotiriou-Leventis, C.; Gao, X.; Leventis, N. *Chem. Commun.* **2001**, 1742.
- (10) Burda, C.; Green, T. C.; Link, S.; El-Sayed, M. *J. Phys. Chem. B* **1999**, *103*, 1783.
- (11) Morrison, S. R. *Electrochemistry at Semiconductor and Oxidized Metal Electrodes*; Plenum Press: New York, 1980.
- (12) Jonsson, M.; Hoummam, A.; Jocy, G.; Wayner, D. D. M. *J. Chem. Soc., Perkin Trans. 2* **1999**, *3*, 425.
- (13) Gaponenko, S. V. *Optical Properties of Semiconductor Nanocrystals*; Cambridge University Press: Cambridge, UK, 1998.
- (14) Klimov, V. I. *J. Phys. Chem. B* **2000**, *104*, 6112.
- (15) Klimov, V.; Hunsche, S.; Kurz, H. *Phys. Rev. B* **1994**, *50*, 8110.
- (16) Hu, Y. Z.; Koch, S. W.; Lindberg, M.; Peyghambarian, N.; Pollock, E. L.; Abraham, F. F. *Phys. Rev. Lett.* **1990**, *64*, 1805.
- (17) Guyot-Sionnest, P. J.; Hines, M. A. *Appl. Phys. Lett.* **1998**, *72*, 686.
- (18) Burda, C.; Link, S.; Mohamed, M.; El-Sayed, M. *J. Phys. Chem. B* **2001**, *105*, 12286.
- (19) Lou, Y.; Chen, X.; Samia, A. C.; Burda, C. *J. Phys. Chem. B* **2003**, *107*, 12431.
- (20) Darugar, Q.; Landes, C.; Link, S.; Schill, A.; El-Sayed, M. *Chem. Phys. Lett.* **2003**, *373*, 284.
- (21) Salvador, M. R.; Hines, M. A.; Scholes, G. D. *J. Chem. Phys.* **2003**, *118*, 9380.
- (22) Micic, O. I.; Jones, K. M.; Cahill, A.; Nozik, A. J. *J. Phys. Chem. B* **1998**, *102*, 9791.
- (23) Micic, O. I.; Sprague, J. R.; Lu, Z.; Nozik, A. J. *Appl. Phys. Lett.* **1996**, *68*, 3150.
- (24) Sant, P. A.; Kamat, P. V. *Phys. Chem. Chem. Phys.* **2002**, *4*, 198.
- (25) van de Lagemaat, J.; Benkstein, K. D.; Frank, A. J. *J. Phys. Chem. B* **2001**, *105*, 12433.
- (26) Pankove, J. I. *Optical Processes in Semiconductors*; Dover Publications: New York, 1975.
- (27) Blackburn, J. L.; Ellingson, R. J.; Micic, O. I.; Nozik, A. J. *J. Phys. Chem. B* **2003**, *107*, 102.
- (28) Kim, S.; Wolters, R.; Heath, J. *J. Chem. Phys.* **1996**, *105*, 7957.
- (29) Leatherdale, C. A.; Kagan, C. R.; Morgan, N. Y.; Empedocles, S. A.; Kastner, M. A.; Bawendi, M. G. *Phys. Rev. B* **2000**, *62*, 2669.